https://doi.org/10.5194/nhess-2019-362
Preprint. Discussion started: 6 January 2020

Natural Hazards and Earth System Sciences
Discussions

Lagrangian Trajectory Modelling for a Person lost at Sea during Adriatic Scirocco Storm of 29 October 2018

Matjaž Ličer[1], Solène Estival[2], Catalina Reyes-Suarez[3], Davide Deponte[3], and Anja Fettich[4]

[1]National Institute of Biology, Piran, Slovenia
[2]École Nationale Supérieure de Techniques Avancées, Paris, France
[3]Istituto Nazionale di Oceanografia e Geofisica Sperimentale, Sgonico, Italy
[4]Slovenian Environment Agency, Ljubljana, Slovenia

Correspondence: Matjaž Ličer (matjaz.licer@nib.si)

Abstract. On 29 October 2018 a windsurfer's mast broke about 1 km offshore during a severe Scirocco storm in the Northern Adriatic Sea. He was drifting in severe marine conditions until he eventually beached alive and well in Sistiana (Italy) 24 hours later. We conducted an interview with the survivor to reconstruct his trajectory and to gain insight into his swimming and paddling strategy. We then attempted a Lagrangian simulation of his trajectory in two ways. Firstly by performing a leeway simulation using the OpenDrift tracking code using two object types: Person-in-Water-1 and Person-powered-vessel-2. Secondly, we model the trajectory using our own Lagrangian tracking code FlowTrack. In both cases a high-resolution (1 km) setup of NEMO v3.6 circulation model was employed for the surface current component and a 4.4 km operational setup of the ALADIN atmospheric model was used for wind forcing. OpenDrift yields best results using Person-powered-vessel-2 object type, indicating a relatively broad search and rescue area which covers 45 km^2 after six hours and rises to 380 km^2 after 24 hours. The simulated most probable SAR area envelops the reconstructed drift trajectory and is also temporaly consistent with the reconstruction. FlowTrack yields a search and rescue area with a comparable lateral extent but with much less downwind spread. While both Lagrangian models were able to envelop the reconstructed drift trajectory during this validation, we recommend using OpenDrift for similar search-and-rescue missions in the future due to its flexibility and drifting object dependent calibration on empirical data.

1 Introduction

Lagrangian particle tracking of objects lost at sea is an important branch of ocean forecasting. Maritime search and rescue (SAR) or other types of civil service responses depend on timely and reliable estimates of the most probable areas which contain the drifting object. These estimates generally require prior computation of ocean currents, waves and winds in the area, which are most often provided by numerical circulation, wave and atmosphere models.

The wind force contribution to the objects drift is termed its leeway and has both downwind (drag) and crosswind (lift) component (Breivik and Allen, 2008). The object's drift therefore generally deviates from the wind direction by some divergence angle L_α (Allen and Plourde, 1999), related to the downwind and crosswind components. Specific values of the object's downwind and crosswind drift are determined by the balance of the wind (lift and drag) force on the overwater part of the object

https://doi.org/10.5194/nhess-2019-362
Preprint. Discussion started: 6 January 2020


Natural Hazards and Earth System Sciences Discussions

and the hydrodynamic (lift and drag) force on the subsurface part of the object - object's drifting properties therefore depend significantly on its shape. Empirical observations have consequently been the most straightforward method of determining the drifting parameters for various drifting object types, including human bodies (Allen and Plourde, 1999; Hackett et al., 2006). Reports on marine drifts involving survivors are not ubiquitous, which makes reviews like (Allen and Plourde, 1999) all the more valuable for any attempt to accurately model the drift of a person or any other object.

In this paper we focus on an incident which occured on 29 October 2018 in the Northern Adriatic Sea and led to a 24 hour drift of a person in gale wind conditions (level 8 on Beaufort scale). For an extensive analysis of the atmospheric and marine conditions during the 29 October 2018 storm the reader is referred to Cavaleri et al. (2019). These conditions are related to the fact that the Adriatic sea is a northwest-southeast oriented elongated basin of the Northern Central Mediterranean, exchanging properties with the eastern Mediterranean basin through the Otranto strait (19° E, 40° N in Figure 1 a)). It is 800 km long and 200 km wide and surrounded from all sides by mountain ridges - the Alps in the north, the Apennines in the west and Dinaric Alps in the east. These ridges exhibit significant influence on the basin circulation through topographic control of the air flow, most notably during episodes of the northeasterly Bora wind and southeasterly Scirocco. The northern part of the Adriatic is a shallow shelf with depths under 60m. Its northernmost part, extending into the Gulf of Trieste, is the shallowest, with depths around 20 to 30m (see Figure 1 b)).

In the afternoon of 29 Oct 2018, the Scirocco speeds along the west coast of northern Istria were in the range 15-25 m s^{-1} and significant wave heights amounted to 3-5 m (Cavaleri et al., 2019), while maximum wave heights in the southern part of the Gulf of Trieste at coastal buoy Vida (see Section 2.1 for details and Figure 1 b) for location) were observed to be over 2.5 m (not shown). The town of Umag in northern Istria is a popular windsurfing spot during Scirocco conditions: on 29 Oct 2018 many people were windsurfing there when the accident occured at estimated 16 UTC. The windsurfer's mast broke roughly 1 km offshore northwest of Umag (see Figure 1 b) for location) initiating the drift. The conditions were too severe for immediate marine rescue either by his colleagues or by authorities. A joint Italian, Croatian and Slovenian SAR mission was initiated next morning (30 Oct 2018) but it was unsuccesful - the surfer beached on his own 24 hours later close to Sistiana north of Trieste (see Figure 1 b)). The windsurfer's harness was however recovered in the central part of the Gulf of Trieste at around 15 UTC on 30 Oct.

The survivor kindly responded to our interview request. We now briefly recapitulate his personal statements about the drift. He was conscious and focused the entire time. The visibility was not bad and he could see the coastline of the Gulf of Trieste in its entirety, which helped him make mental notes of his location. His mast broke on 29 Oct 2019 16 UTC at 13.625° E, 45.558° N with an estimated $\pm$500 m error in each direction, see Figure 1 b) for location.

Immediately after the accident, he drifts alongshore north of Umag and he actively paddles towards the coast, hoping to reach the Cape of Savudrija. The wind direction at his location is however slightly offshore and sometime between 19.30 and 20.30 UTC he realizes he will not be able to reach Savudrija. He releases his windsurfing harness in the water. After 20 UTC the Scirocco strengthens. He is now located northwest of Savudrija, drifting north-northwest toward Grado. Swimming is not possible due to airspray and sea conditions, but he keeps shaking his arms and legs interchangeably to keep warm. At some point between 20 UTC and 23 UTC he can see the town of Izola (Slovenia) and the town of Grado (Italy) at right angles.

https://doi.org/10.5194/nhess-2019-362
Preprint. Discussion started: 6 January 2020

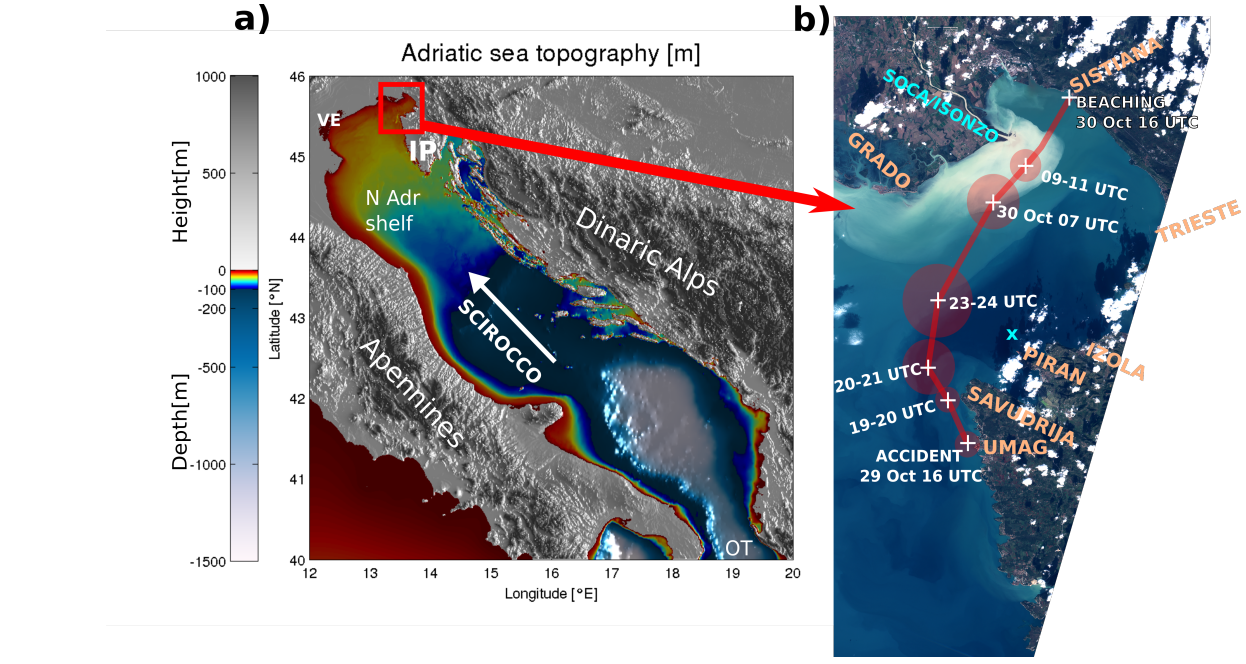

Figure 1. a) Adriatic basin bathymetry. Abbreviations are as follows: VE - Venice, IP - Istrian Peninsula, N Adr Shelf - Northern Adriatic Shelf, OT - Otranto Strait. Direction of Scirocco is marked with white arrow. b) The Gulf of Trieste and piecewise trajectory of the drift as estimated by the survivor. Location estimates are junctions of the piecewise straight line. Circles denote location uncertainty estimates at specific times. The cyan 'x' sign north of Piran denotes the location of the Vida coastal buoy. Background layer is Sentinel-2 L1C True Color image of the Gulf of Trieste from the day after the beaching, 31 Oct 2018 (obtained from Copernicus Open Access Hub: https://scihub.copernicus.eu). Turbid Soča/Isonzo river plume is clearly visible along the northern shore of the Gulf.

It is around 23 UTC that his drift turns north-east. After 23 UTC, he is located approximately on the Piran-Grado line. Sea conditions get very severe, he is laying on the windsurf board, mostly facing southwest, away from the mean drift direction, drifting backwards, clutching the footstraps on the surfboard. He estimates that every 50th wave breaks over him and pulls the surfboard from under him. When this happens he needs to wait to reach the crest of the wave to re-locate the board and catch it. In the morning, on 30 Oct 2019 07 UTC, he is located 2 - 4 km south-southwest of the Soča/Isonzo river mouth. By 9-10 UTC he is located roughly 1-2 km south-southeast of the river mouth and the water gets significantly colder as he likely enters the Soča/Isonzo river plume (visible in Figure 1 b)). By the time of his entering the plume, the Soča/Isonzo runoff is at a several-month maximum, as depicted in Figure 2. From 11 UTC on he is paddling actively toward northeast to overcome the riverine westward coastal current until he reaches the beach near Sistiana at 16 UTC.

The drifting trajectory, reconstructed from above, is shown in the b) panel in Figure 1. In the present paper, we present two attempts to simulate this trajectory using two different particle tracking models, OpenDrift and FlowTrack. Available observations and general marine conditions during the drift are presented in Section 2; numerical models used for particle

https://doi.org/10.5194/nhess-2019-362
Preprint. Discussion started: 6 January 2020

Natural Hazards and Earth System Sciences
Discussions

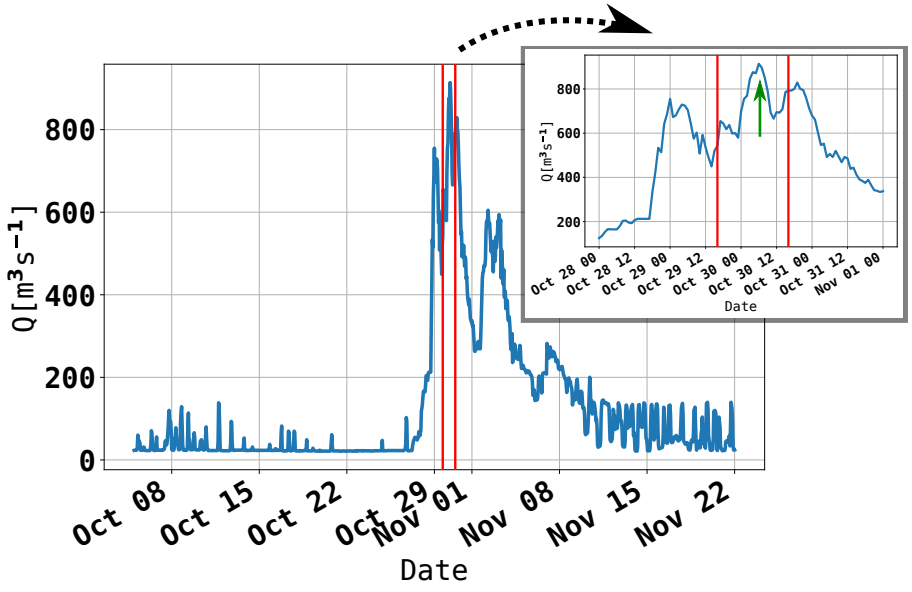

Figure 2. Soča/Isonzo runoff during October and November 2018, as measured at an upstream river gauge (operated by ARSO) at Solkan, Slovenia. Vertical red lines indicate the timewindow of the drift. Green arrow in the inset marks approximate time of windsurfer's entering the river plume.

tracking are described in Section 3. Lagrangian models are presented in Section 4. Simulation results are depicted and discussed in Section 5, followed by concluding remarks in Section 6.

2 Observations

2.1 Coastal buoy Vida

The oceanographic buoy Vida is a coastal observation platform, operated by the Marine Biology Station at the National Institute of Biology (NIB). It is located in the southern part of the Gulf of Trieste at (13.55505 E, 45.5488 N), see b) panel of Figure 1 (marked with a cyan cross). Data from the buoy are multifaceted (air temperature, air humidity, currents, waves, sea temperature, salinity, dissolved oxygen, chlorophyll concentration, etc.) and are publicly available (http://www.nib.si/mbp/en/buoy/) in near real time. Ocean currents are acquired by a Nortek AWAC acoustic Doppler current profiler, mounted on the sea bottom at a depth of 22.5 m, to monitor vertical current profiles (at 1 m intervals along the water column). The top most cell of the ADCP measurement corresponds to a depth around 0.5 m. Further information on the buoy can be found in Malačič (2019).

https://doi.org/10.5194/nhess-2019-362
Preprint. Discussion started: 6 January 2020


Natural Hazards and Earth System Sciences
Discussions

2.2 High Frequncy Radar System

The HF systems deployed in the Gulf of Trieste consist of two WERA stations (Gurgel et al., 1999) manufactured by Helzel MessTechnik in Germany, one at the OGS facility in Aurisina (Italy) and the second, operated by NIB, in the urban area of Piran (Slovenia). The systems provide sea surface current maps since January 2015. They rely on the scattering of a short-duration (9 minutes) and low-power (below 20 Watts) harmless radio wave pulses from waves at the ocean surface satisfying the Bragg-resonance scattering condition for coherent return. The two systems operate at a carrier frequency of 25.5 MHz as regulated by the International Telecommunication Union, covering the Gulf of Trieste at 1 km range resolution and 1° angular resolution every 30 minutes. After aquisition, data are processed and radial components of the surface current field are obtained, which in turn are combined into a 1.5 km horizontal resolution 22×20 regular grid (see Figure 5 for coverage during the event and both station locations). Combined data are stored in databases and can be visualized in near real time at http://www.nib.si/mbp/en/oceanographic-data-and-measurements/other-oceanographic-data/hf-radar-2. The two WERA HF systems are operated and maintained in collaboration between researchers, engineers and technicians from OGS and NIB.

3 Models

3.1 Ocean, Wave and Atmospheric Models

3.1.1 NEMO Circulation Model

We are using a high horizontal resolution (1°/111 or roughly 1000 m) setup of NEMO v3.6 (Madec, 2008) over the Adriatic basin on a regular 999×777 longitude-latitude grid and 33 vertical z^*-levels with partial step. Model domain spans $12°-21°$ E and $39°-46°$ N, see Figure 3. Maximum vertical discretization stretch is located at 15th level to allow for appropriate vertical resolution near the surface. In all regions shallower than 2 m, a minimum 2 m depth is enforced. Vertical level depths in meters are 0.50, 1.51, 2.55, 3.64, 4.83, 6.20, 7.94, 10.38, 14.18, 20.56, 31.68, 51.23, 84.58, 137.94, 215.83, 318.24, 440.67, 576.90, 721.55, 870.95, 1022.92, 1176.25, 1330.29, 1484.69,1639.28, 1793.97, 1948.71, 2103.47, 2258.25, 2413.03, 2567.81, 2722.60, 2877.39. Explicit time-splitting is enforced and barotropic timestep is automatically adjusted to meet Courant-Friedrichs-Lewy stability criterion. Baroclinic timestep was set to 120 s. The model is hotstarted daily from previous operational run. Hourly lateral boundary conditions in the Ionian Sea are taken from the Copernicus CMEMS MFS model. Turbulent heat and momentum fluxes across the ocean surface are computed with CORE bulk flux formulation (Large and Yeager, 2004) using ALADIN SI atmospheric fields (surface wind, cloud cover, mean sea level pressure, 2m temperature, relative humidity and precipitation). Rivers are implemented as freshwater release over the entire water column at the discharge location, with runoff values as described in Ličer et al. (2016). Tides are included as lateral boundary conditions for open boundary elevations and barotropic velocities for K1, P1, O1, Q1, M2, K2, N2 and S2 constituents. Constituents at the open boundary are obtained using OTIS tidal inversion code (Egbert and Erofeeva, 2002), based on TPXO8 atlas. The model employs Flather boundary condition for barotropic dynamics and Flow Relaxation Scheme (Engedahl, 1995) for baroclinic dynamics and tracers at the

https://doi.org/10.5194/nhess-2019-362
Preprint. Discussion started: 6 January 2020

Natural Hazards and Earth System Sciences
Discussions

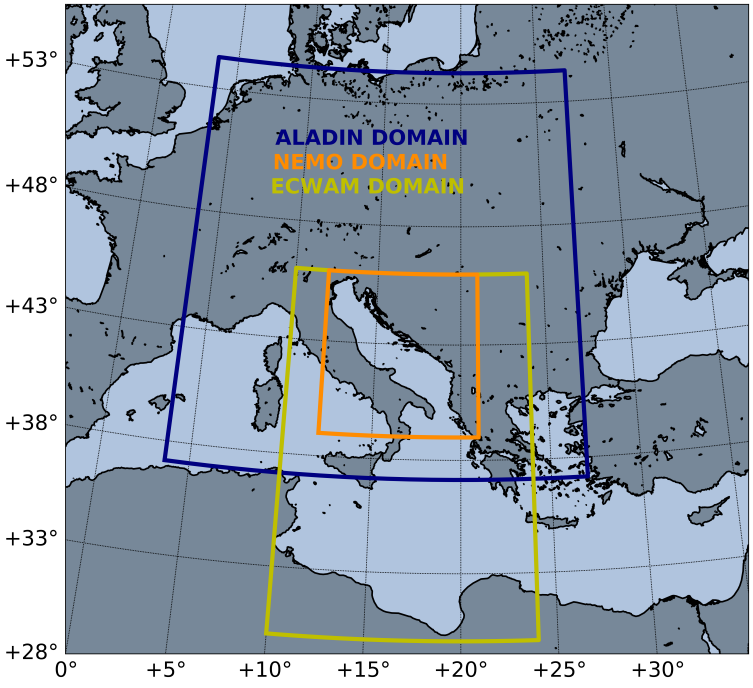

Figure 3. Computational domains of ALADIN SI (blue), NEMO (orange) and ECWAM (olive) numerical models.

open boundary. Lateral momentum boundary condition at the coast is free-slip. Bottom friction is nonlinear with a logarithmic boundary layer. Lateral diffusion schemes for tracers and momentum are both bilaplacian over geopotential surfaces. Vertical diffusion is computed using Generic Length Scale (GLS) turbulence scheme. Craig and Banner formulation (Craig and Banner, 1994) of surface mixing due to wave breaking is switched on.

3.1.2 ECWAM Wave Model

The wave model used in this study is running operationally at Slovenian Weather Service. It is a regional setup of ECWAM cycle 46R1 code (full documentation is available at https://www.ecmwf.int/sites/default/files/elibrary/2018/18717-part-vii-ecmwf-wave-model.pdf) on a regular (1°/60) longitude-latitude grid. Model domain spans $10° - 24°$ E and $30° - 46°$ N, see Figure 3. The model uses 25 frequency bins and 36 direction bins. Since the ECWAM domain extends south to the north African coast (to capture the swell from Central Mediterranean during Scirocco episodes), we provide wind forcing as a hybrid of ALADIN SI and ECMWF operational global forecast surface winds. ALADIN SI surface winds are used as forcing over the Adriatic basin, while ECMWF fields are used in the central Mediterranean outside of the ALADIN domain. A linear interpolation is applied over 5 cells to reduce wind gradients between the two products. It is worth noting that the ALADIN SI model is forced at the boundary by the same ECMWF product we use to provide winds to ECWAM outside (and south of) the ALADIN domain. Computational timesteps are 45 s for the propagation and 360 s for the source function. A second order

https://doi.org/10.5194/nhess-2019-362
Preprint. Discussion started: 6 January 2020


Natural Hazards and Earth System Sciences
Discussions

propagation scheme is used. Deep water approximation is not enforced. No lateral boundary conditions are enforced at the eastern and western lateral open boundary. The latter is acceptable since the waves provided at the lateral boundaries cannot propagate into the Adriatic, which is our primary domain of interest, see Figure 3.

3.1.3 ALADIN Atmospheric Model

The version of the model used for the experiments in this paper is currently operational at the Slovenian Weather Service. It runs on a 432×432 horizontal Lambert conic conformal grid with 4.4 km resolution and 87 vertical levels with the model top at 1 hPa and model integration time step of 180 s. The model domain spans $[0.7^\circ\,\mathrm{W}, 28.6^\circ\,E]$ in longitude and $[37.4^\circ\,\mathrm{N}, 55.0^\circ\,\mathrm{N}]$ in latitude, see Figure 3. The physics package used in the model is the so-called ALARO-0, that uses Modular, Multi-scale, Microphysics and Transport (3MT) structure (Gerard et al., 2009). Initial conditions for the model are provided by atmospheric analysis with 3 hourly three-dimensional variational assimilation (3D-Var) (Fischer et al., 2005; Strajnar et al., 2015) and optimal interpolation for surface and soil variables. Sea surface temperature (SST) in the model is initialized from the most recent host model analysis of the ECMWF model that uses Operational Sea Surface Temperature and Sea Ice Analysis (OSTIA, Donlon et al., 2012), supplied by the National Environmental Satellite, Data and Information Service (NESDIS) of the American National Ocean and Atmospheric Administration (NOAA). Information at the domain edge is obtained from the global model by applying Davies relaxation (Fischer et al., 1976). Lateral boundary conditions are provided by the ECMWF Boundary Conditions Optional project and are applied with a 1 h period in the assimilation cycle and a 3 h period during model forecasts. Boundary condition information is interpolated linearly for time steps between these times. Further details about the model setup and assimilation scheme are available in Strajnar et al. (2015); Ličer et al. (2016).

4 Particle Tracking Models

4.1 OpenDrift Model and Setup

OpenDrift is an open-source Python-based Lagrangian particle modelling code developed at the Norwegian Meteorological Institute with contributions from the wider scientific community. It is described in detail in Dagestad et al. (2018). It supports a wide range of offline (i.e. with precomputed currents and winds) predictions from oil spills and drifting objects to microplastics and fish larvae transport. Particle seeding is very convenient to use and its Leeway module supports a wide range of object types with different lift and drag behaviour under current and wind forces (Dagestad et al., 2018). Object drift is decomposed into downwind and crosswind components (Breivik and Allen, 2008) based on empirical observations collected in Allen and Plourde (1999).

The object types used in this study were of two types. First drift object type was Person-in-water (PIW-1), corresponding to empirically determined (Allen and Plourde, 1999) downwind slope of 1.93 %, downwind standard deviation of 0.083 m s^{-1}, right slope of 0.51 %, right standard deviation of 0.067 m $s^{-}1$, left slope of -0.51 % and left standard deviation of 0.067 m s^{-1}. Second object type was PERSON-POWERED-VESSEL-2 (Surf board with person), corresponding to empirically determined

https://doi.org/10.5194/nhess-2019-362
Preprint. Discussion started: 6 January 2020

Natural Hazards and Earth System Sciences
Discussions

(Allen and Plourde, 1999) downwind slope of 0.96 %, downwind standard deviation of 0.12 m s^{-1}, right slope of 0.54 %, right standard deviation of 0.094 m $s^{-}1$, left slope of -0.54 % and left standard deviation of 0.067 m s^{-1}). The simulation was run in both cases for 31 hours using a second order Runge-Kutta scheme. Forcing data consisted of NEMO currents and ALADIN SI 10m winds from the 00 UTC operational runs of both models, performed on 29 Oct 2019 at the Slovenian Environment Agency.

4.2 FlowTrack Model and Setup

FlowTrack is an offline individual-based Lagrangian tracking model, developed for the general purpose tracking problems from marine oil-spill dispersion modelling to water age, marine bacterial transport and object drift forecasting. The model was written by one of the authors (M. L.) in Fortran 95 with shared memory (openMP) parallelization. An arbitrary number of particles N_p (i.e. several thousand) are allowed. In this study $N_p = 408$ particles were seeded in a 1 km $\times$1 km square around the initial location. Once the particle is initialized in the wet cell of the model grid, it is subjected in each timestep to advection, turbulent diffusion and, if applicable, fate. Lagrangian trajectory $\mathbf{r}_p(t)$ of $p-$th particle ($p = 1, \ldots, N_p$) is computed using a second order Runge-Kutta method (Euler method is also available) to integrate the following initial value problem

$$\frac{d\mathbf{r}_p(t)}{dt} = \mathbf{u}_c(\mathbf{r}_p(t),t) + q \cdot \mathbf{u}_{w,p}(\mathbf{r}_p(t),t) + \mathbf{u}_s(\mathbf{r}_p(t),t) + \mathbf{u}' \quad (1)$$

$$\mathbf{r}_p(0) = \mathbf{r}_{0,p} \quad (2)$$

where $\mathbf{r}_{0,p}$ in Equation (2) denotes initial position of p-th particle.

Terms of the right hand side of equation (1) are as follows. Term $\mathbf{u}_c(\mathbf{r}_p(t),t)$ denotes the Eulerian current at particle location $\mathbf{r}_p(t)$ at time t. This term is obtained from the NEMO circulation model. Term $\mathbf{u}_{w,p}(\mathbf{r}_p(t),t)$ denotes the wind drift vector of the p-th particle at particle location $\mathbf{r}_p(t)$ at time t. Wind drift generally has lift and drag component, thus deviating from the wind direction. This deviation is treated in FlowTrack by rotating the wind drift vector of p-th particle by an angle $\theta(p) \in [-L_\alpha, +L_\alpha]$, where L_α stands for the leeway divergence angle (Allen and Plourde, 1999). In this work L_α was set to 20° as recommended for a person with surfboard in Table 8-1 of Allen and Plourde (1999). Since wind lift can generally act to the left or to the right of wind, with both options having equal probabilities (Breivik and Allen, 2008), FlowTrack distributes $\theta(p)$, where $p = 1, \ldots, N_p$, linearly over the $[-L_\alpha, +L_\alpha]$ interval, namely

$$\theta(p) = -L_\alpha + \frac{p-1}{N_p - 1} \cdot 2L_\alpha \,. \quad (3)$$

Each particle retains its respective angle of rotation throughout the simulation and does not jibe. The wind drift vector of the p-th particle is then computed from ALADIN SI 10m winds $\mathbf{u}_{10}(\mathbf{r}_p(t),t)$ at particle location as

$$\mathbf{u}_{w,p}(\mathbf{r}_p(t),t) = \begin{bmatrix} \cos\theta(p) & -\sin\theta(p) \\ \sin\theta(p) & \cos\theta(p) \end{bmatrix} \cdot \mathbf{u}_{10}(\mathbf{r}_p(t),t) \,. \quad (4)$$

Parameter q in equation (1) scales the object's drift speed to the wind speed. It was estimated from OpenDrift empirical coefficients mentioned in the previous sections as follows. Downwind drift scales as $q_{DW} = 1.93$ % of the wind speed. The

https://doi.org/10.5194/nhess-2019-362
Preprint. Discussion started: 6 January 2020


Natural Hazards and Earth System Sciences
Discussions

downwind standard deviation is 0.083 m s^{-1}, which at 15 m s^{-1} (i.e. typical wind speed during the event) amounts to $q^{\sigma}_{DW} = 0.4$ %. The crosswind components in OpenDrift scale as $q_{XW} = 0.51$ % of the windspeed, with standard deviations of 0.067 m s^{-1}, which at 15 m s^{-1} amounts to $q^{\sigma}_{XW} = 0.34$ %. Since mere rotation of the wind drift vector, applied in FlowTrack, does not alter its modulus, and hence disregards the wind lift force, we attempted to compensate for this by estimating $q = \sqrt{(q_{DW} + q^{\sigma}_{DW})^2 + (q_{XW} + q^{\sigma}_{XW})^2} \approx 2.5$ percent of the wind speed.

Term $\mathbf{u}'$ in (1) represents random fluctuations in the velocity vector to simulate subgrid turbulent diffusion. In the present paper, the modulus of fluctuations has been manually constrained to $2 \cdot 10^{-2}$ m s^{-1}. Term $\mathbf{u}_s(\mathbf{r}_p(t), t)$ on the right hand side of the equation (1) is the Stokes drift contribution, i.e. Eulerian mean of unclosed Lagrangian particle orbits in the surface gravity wave field. It was however shown (see (Hackett et al., 2006; Breivik and Allen, 2008) for further references) that Stokes drift, while present in the motion of the water, has negligible impact on drift speed of objects whose typical dimension is more than roughly six times smaller than surface gravity wave wavelength λ_w. We can compute λ_w from surface gravity wave dispersion relation $\omega(k) = \sqrt{gk \tanh(kH)}$. Since wave vector is $k = 2\pi/\lambda_w$, we can solve for λ_w by iterating

$$\lambda_w = \frac{gT_w^2}{2\pi} \tanh \frac{2\pi H}{\lambda_w} \tag{5}$$

where T_w is the mean wave period of the wave field obtained from the ECWAM model at a representative point along the particle trajectory during the 29 Oct 2018 storm, g is acceleration due to gravity and H is the undisturbed ocean depth. Within the drifting area surface gravity wave wavelengths during the 29 Oct 2018 storm exceeded 50-70 m. Since the surfboard is roughly 3 m long, Stokes drift effect can be safely ignored, which simplifies initial value problem (1)-(2) to

$$\frac{d\mathbf{r}_p(t)}{dt} = \mathbf{u}_c(\mathbf{r}_p(t), t) + q \cdot \begin{bmatrix} \cos\theta(p) & -\sin\theta(p) \\ \sin\theta(p) & \cos\theta(p) \end{bmatrix} \cdot \mathbf{u}_{10}(\mathbf{r}_p(t), t) + \mathbf{u}' \tag{6}$$

$$\mathbf{r}_p(0) = \mathbf{r}_{0,p}\,. \tag{7}$$

In situations where Stokes drift is not negligible, FlowTrack is currently adapted for use with Stokes drift field from ECWAM cycle 46R1, but generalization to any other wave model whose Stokes drift results can be remapped to a regular longitude-latitude grid is trivial. Forcing data to FlowTrack is identical to the one of OpenDrift, and consisted of NEMO currents and ALADIN SI 10m winds from the 00 UTC operational runs of both models, performed on 29 Oct 2019 at the Slovenian Environment Agency.

5 Results and Discussion

In this section we present a qualitative analysis of marine conditions from available observations, and also marine drift results from both particle tracking models presented in Section 4.

Figure 4 depicts wind measurements and ALADIN SI modelled winds at the Vida coastal buoy (12 km northeast of the accident location, see Figure 1 b).) for the timewindow 29 - 31 Oct 2019. Qualitatively there is a very solid agreement between the two timeseries. Measured wind at Vida exhibits southeasterly 140° direction in the hours after the accident (left dashed line

https://doi.org/10.5194/nhess-2019-362
Preprint. Discussion started: 6 January 2020

Natural Hazards and Earth System Sciences
Discussions
Open Access
EGU

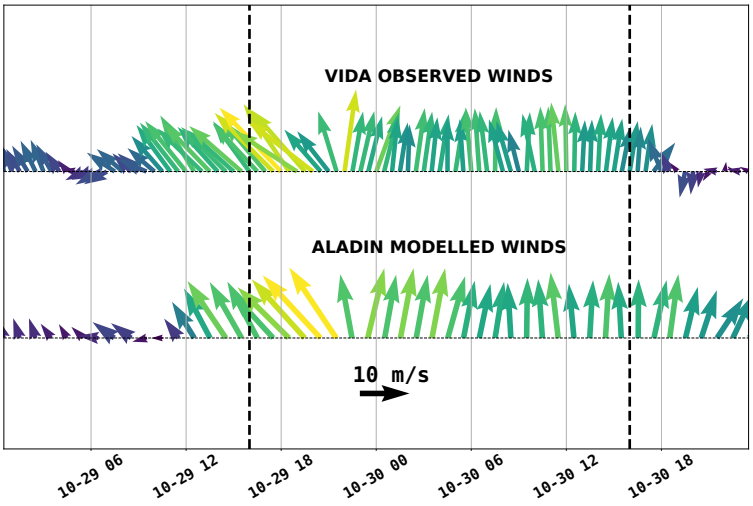

Figure 4. Arrow plots of observed and ALADIN SI modelled wind directions at Vida coastal buoy during 29 Oct 2018 event. Drift period is marked with dashed vertical lines. Arrows are colored by their wind speed.

in Figure 4), followed by a shift to slight south-southwest 190° between 30 Oct 00 UTC and 04 UTC, and finally a southerly 180° direction during the day. (All directions in the paper are stated in nautical notation, i.e. 0° marking north, 90° marking east.) Wind speed is constantly around 15 - 20 m s^{-1}.

HF observations in Figure 5 are presented as a qualitative check for the NEMO model surface currents during the 24 hours of the drift. HF measurements and modeled currents both exhibit eastward topographically constrained coastal current in the northern part of the Gulf between Grado and Soča/Isonzo rivermouth, with NEMO tending to underestimate observations (as shown below however, wind drift was the main contribution to the drift). Absence of the coastal current on Oct 29th 22 UTC might be related to the model treatment of high Soča/Isonzo discharge, which in itself generates westward inertial current in that part of the modelling domain, and might be counteracting wind driven (eastward) currents. On the other hand both the model and the HF measurements indicate that the surface layer on Oct 29th 22 UTC was wind dominated, exhibiting an inflow over most of the surface area of the Gulf, see also (Malačič et al., 2012).

Another common feature of NEMO currents and HF radar observations is the general anticyclonic character of the surface circulation through the rest of the night and the following day. This is in contrast with the Northern Adriatic basin-scale cyclonic current pattern during Scirocco episodes (not shown) and stems from the fact that Scirocco induced surface currents, flowing north along the Istrian coast, typically branch upon hitting the northern end of the Adriatic basin. The eastward branch of this wind driven current inflows into the Gulf of Trieste along the northern coastline. Such inflow, visible in modeled and observed currents is therefore not unexpected during Scirocco episodes. As is further shown in Figure 6, *in situ* currents measured at Vida buoy also exhibit a westward direction over the entire water column during the timewindow of the drift, and are therefore consistent with the overall anticyclonic character of the surface circulation, exhibited in the model and radar surface current

https://doi.org/10.5194/nhess-2019-362
Preprint. Discussion started: 6 January 2020

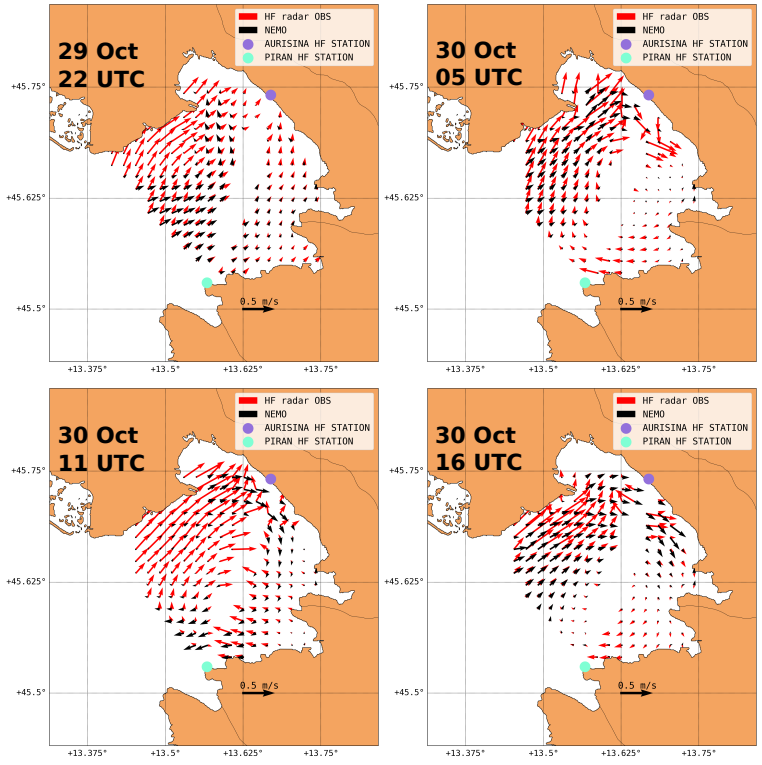

Figure 5. HF radar measurements in the Gulf of Trieste during the period of the drift. Since there are gaps in surface current measurements, the closest observations to 29 Oct 22 UTC and 30 Oct 04, 10, 16 UTC are depicted. NEMO currents were bilinearly interpolated to WERA grid points. Arrow lengths from both fields are commonly scaled.

maps. NEMO model underestimation of the observed surface currents will however need to be thoroughly addressed in further investigations.

Figure 7 depicts current and wind drift inputs to both models over the period of the windsurfer's drift.The wind drift seems to be the dominant driving factor of the windsurfer's drift, its speed being roughly double that of the surface currents. Wind drift prior to (not shown) and at 22 UTC has a clear southeasterly direction (at Umag - offshore) at roughly 140-160°, consistent with the windsurfer's experience and his inability to reach Savudrija in time. During the night the wind direction shifts into a south-southwesterly to about 190°, also consistent with his experience. In the morning of 30 Oct 2018 and through the day, the wind direction is predominantly southern at 180°. This is all in agreement with the direction shift measured at Vida buoy (Figure 4).

NEMO currents at 22 UTC indicate northward direction along the coast of Istria and also a surface inflow along all but the northernmost part of the opening of the Gulf of Trieste. The northernmost part along the northern coast of the Gulf most

https://doi.org/10.5194/nhess-2019-362
Preprint. Discussion started: 6 January 2020

Natural Hazards and Earth System Sciences
Discussions

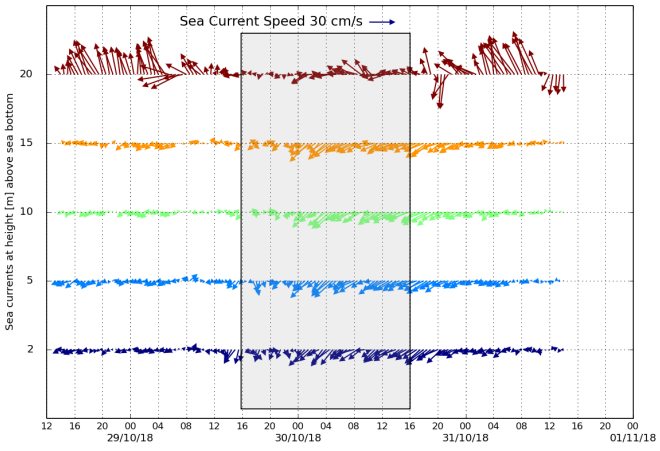

Figure 6. Arrow plot of ADCP measurements of ocean currents at Vida coastal buoy during 29 Oct 2018 event (shaded rectangle delimits the time window of the drift). Surface current timeseries is plotted in the top line.

likely shows no notable inflow due to inertial westward coastal current from the Soča/Isonzo river, which manifests itself as an outflow from the Gulf, confined to this part of the coast (see Figure 1 for the related river plume).

OpenDrift results for drifting object type Person in Water (PIW-1) are presented in Figure 8. Figure shows 6-hourly snapshots of particles, initially seeded in the green region at 29 Oct 2019 16 UTC. After 6 hours, at 22 UTC, roughly 75 percent of particles are still in the water column, with the majority of the particles lagging behind the estimated windsurfer location. Particles at the northern forefront seem however to be well in the region of where the windsurfer estimated his position between 20 UTC and 23 UTC. The search and rescue area after 6 hours amounts to estimated 70 km^2 (this estimate is made by computing the area of a polygon, determined by locations of the outermost group of particles).

Shift in the wind direction from southeast to south-southwest (see Figure 4), occuring sometime after 29 Oct 22 UTC and lasting until 04 UTC, causes a corresponding shift in particles' drifting directions. The envelope of particles' trajectories fully contains the reconstructed trajectory. The search and rescue area after 12 hours amounts to roughly 240 km^2.

First particles are beaching on the northern shore of the Gulf between 04 UTC and 10 UTC. This predominantly occurs between Grado and the Soča/Isonzo river mouth. Particles in the Gulf are propagating along the reconstructed trajectory, but with increasing lateral and axial extent: search and rescue area after 18 hours amounts to estimated 500 km^2. After 24 hours several ($>$10) particles beach within 2 km of the actual beaching location. Search and rescue area at this point consists of most of the Gulf of Trieste, covering 650 km^2.

OpenDrift results for drifting object type PERSON-POWERED-VESSEL-2 (Surf board with person) are presented in Figure 9. After 6 hours, at 22 UTC, roughly 90 percent of particles are still in the water column, with the majority of the particles centered around the estimated windsurfer location. After 12 hours, at 04 UTC, the envelope of the particles seems to be lagging

https://doi.org/10.5194/nhess-2019-362
Preprint. Discussion started: 6 January 2020

Natural Hazards and Earth System Sciences
Discussions
Open Access
EGU

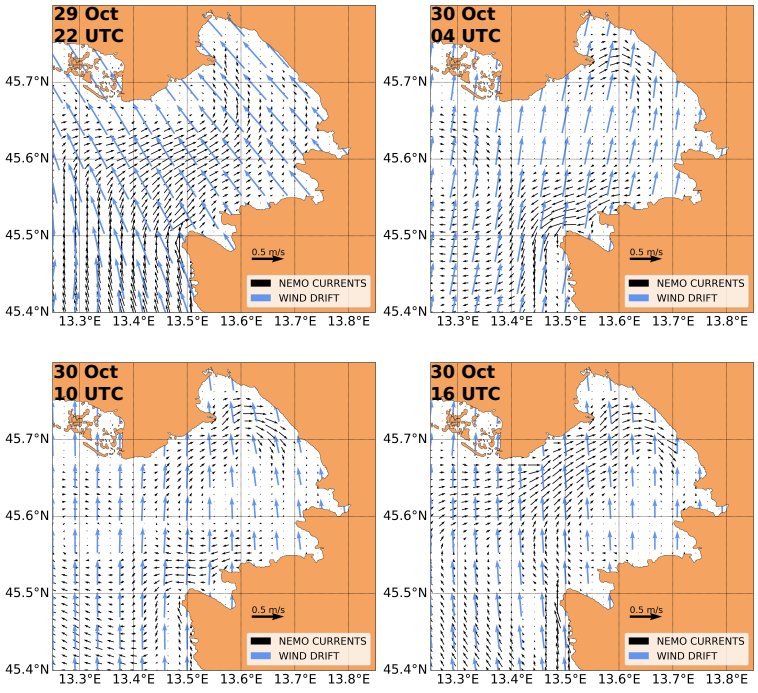

Figure 7. 6-hourly same-scale snapshots of NEMO currents (black arrows) and ALADIN SI 10m wind induced wind drift (blue arrows) over the period of the windsurfer's drift. Only purely downwind arrows with no departure from the ALADIN SI wind velocity vector are plotted. Only every third wind point is plotted for clarity. Arrow lengths from both fields are commonly scaled.

a few hours behind - they are centered at the 23-24UTC estimate of the surfers position. The forefront of the particle distribution however contains the estimated trajectory at all times. The search and rescue area after 6 hours amounts to estimated 45 km^2 (this estimate is made by computing the area of a polygon, determined by locations of the outermost group of particles). The search and rescue area after 12 hours in this case amounts to roughly 160 km^2.

First particles are beaching on the northern shore of the Gulf between 04 UTC and 10 UTC. This predominantly occurs between Grado and the Soča/Isonzo river mouth. Particles in the Gulf are propagating along the reconstructed trajectory, but with increasing lateral and axial extent: search and rescue area after 18 hours amounts to estimated 250 km^2. After 24 hours several ($>$10) particles beach within 2 km of the actual beaching location. Search and rescue area at this point consists of the northern half Gulf of Trieste, covering 380 km^2.

Simulations using object type PERSON-POWERED-VESSEL-2 yield smaller SAR areas which are more consistent with the survivor's trajectory estimate than SAR areas based on PIW-1 object type. While one can clearly benefit from using the most appropriate drift parametrization, lack of information during an actual event often complicates the decision on which parametrization to use.

https://doi.org/10.5194/nhess-2019-362
Preprint. Discussion started: 6 January 2020

Natural Hazards and Earth System Sciences
Discussions
Open Access
EGU

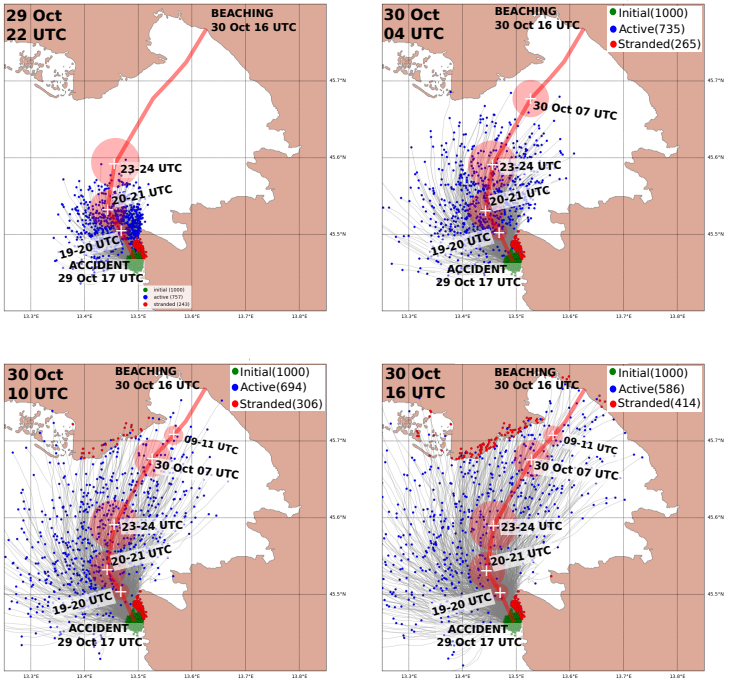

Figure 8. OpenDrift simulation of the Person in Water (PIW-1) object type. Lagrangian drift is depicted every 6 hours after the accident (green dots mark the initial seeding location) on 29 Oct 2019 16 UTC. Red line denotes trajectory of the drift, as reconstructed by the survivor. White crosses denote locations at specific times, while red circles around crosses denote uncertainty estimates of the respective location estimates.

Simulation results from FlowTrack model are presented in Figure 10. One shortcoming of this model is immediately clear: the model currently lacks properly calibrated, object dependent diffusion both in and across the propagation direction. Particles (initially seeded in a rectangular region around the accident location) consequently spread mostly laterally due to the variability in leeway divergence angle $\theta(p)$. With wind drift being the dominant factor, the overall envelope of particle trajectories correlates with the one from OpenDrift, but with somewhat narrower lateral extent. Consequently, and unlike OpenDrift, FlowTrack can at present give no useful quantitative estimate of the search and rescue area.

The simulation trajectory is also temporally consistent with the reconstructed trajectory - particles in the vicinity to the reconstructed trajectory do not significantly lag or overtake windsurfer's location estimate. The reconstructed trajectory is however located more or less on the eastern outer edge of all simulated routes and represents more of an outlying scenario than in the case of OpenDrift.

https://doi.org/10.5194/nhess-2019-362
Preprint. Discussion started: 6 January 2020

Natural Hazards and Earth System Sciences
Discussions

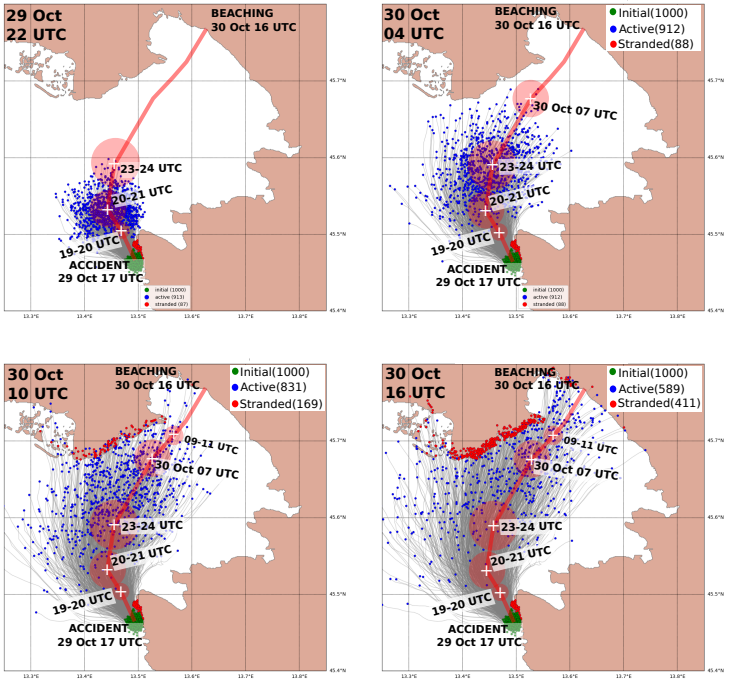

Figure 9. OpenDrift simulation of the PERSON-POWERED-VESSEL-2 object type. Lagrangian drift is depicted every 6 hours after the accident (green dots mark the initial seeding location) on 29 Oct 2019 16 UTC. Red line denotes trajectory of the drift, as reconstructed by the survivor. White crosses denote locations at specific times, while red circles around crosses denote uncertainty estimates of the respective location estimates.

6 Conclusions

In the paper we present a modeling analysis of the 24-hour marine drift by the windsurfer whose mast broke on 29 Oct 2018 16 UTC, during a 29 Oct 2018 Scirocco storm in the Northern Adriatic. We conduct an interview with the survivor in order to reconstruct his trajectory and its uncertainty. We present numerical circulation (NEMO), wave (ECWAM), atmosphere (ALADIN SI) and Lagrangian tracking models, used in an attempt to hindcast this trajectory. We present available measurements from the regional coastal buoy Vida and HF surface current radar to qualitatively assess marine conditions in the Gulf of Trieste during the period of the drift.

Two Lagrangian tracking models were employed to compute the survivor's trajectory. First was OpenDrift, an established open source Lagrangian model, ingesting ocean currents and winds, and using past observational data to compute the drift of objects in marine environment. Neither Stokes drift nor wave data are explicitly included in OpenDrift input data since these effects are already present in the downwind/crosswind drift parametrizations, deduced from observations.

The second Lagrangian tool was FlowTrack, a general purpose individual-based particle tracking model, written for Lagrangian tracking, water age and oil spill modelling in a marine environment. FlowTrack in principle allows for ingestion of

https://doi.org/10.5194/nhess-2019-362
Preprint. Discussion started: 6 January 2020

Natural Hazards and Earth System Sciences
Discussions

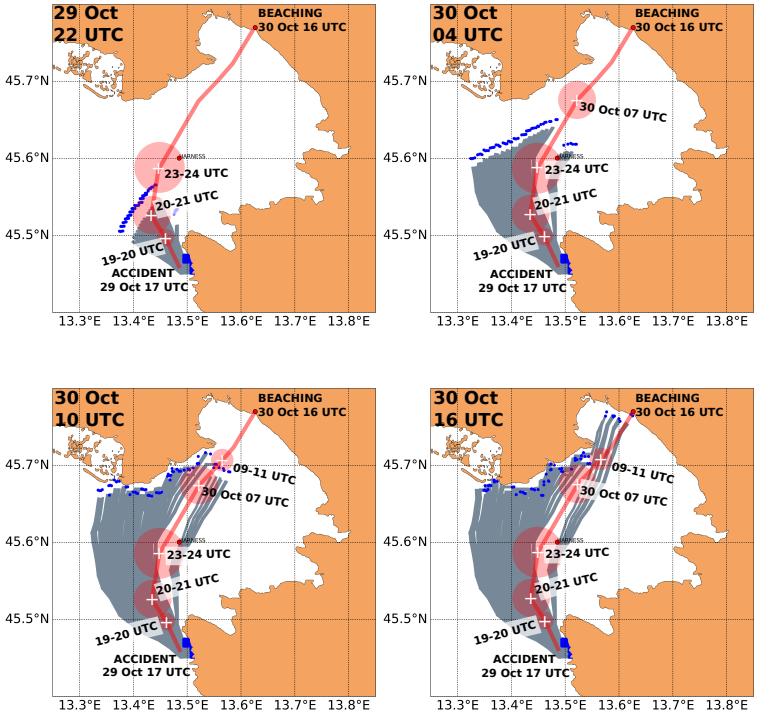

Figure 10. Same as Figure 8, but for a FlowTrack simulation of the windsurfer's drift. Location of harness recovery is marked with a red circle at (13.48 E, 45.6 N).

wave data and Stokes drift computation prior to particle advection, but this option was not used for the simulations performed in this paper. The reason for this is that wave-induced drift has been shown to be of importance only for objects whose typical dimension is comparable to the wavelength of surface gravity waves scattering off the object. During the storm in question, surface gravity waves wavelengths surpassed 50 m, a value ten to twenty times longer than the length of the board or a person.

OpenDrift simulation were performed using two object types (PIW-1 and PERSON-POWERED-VESSEL-2), both indicating a rapidly growing search area which however extended along the reconstructed trajectory of the survivor's drift. The trajectories in both cases are spatially and temporally consistent with the reconstruction, but PERSON-POWERED-VESSEL-2 was more consistent with the survivor's trajectory estimate and yielded smaller and more precise SAR areas. Based on OpenDrift results, 6 hours after the incident the search area spans 70 (45) km^2, rising more or less linearly to 650 (380) km^2 after 24 hours for PIW-1 (PERSON-POWERED-VESSEL-2) object type. This merely confirms that search and rescue response should be as rapid as possible.

FlowTrack simulation currently lacks the capability of estimating the search and rescue area due to lack of downwind diffusion. Particle trajectories from FlowTrack are nevertheless defining an envelope within which the reconstructed trajectory takes place. The timing of the eventual beaching is also valid to within 3 hours.

https://doi.org/10.5194/nhess-2019-362
Preprint. Discussion started: 6 January 2020


Natural Hazards and Earth System Sciences
Discussions

316 Nevertheless we find the OpenDrift approach better grounded for decision support during future search and rescue opera-
317 tions. Its downwind/crosswind parametrizations are based in observations and yield object class dependent search and rescue
318 area. FlowTrack currently lacks any object class parametrization and simulations performed in this paper required constrain-
319 ing modeling parameters using existing literature. This is typically not temporally feasible during actual search and rescue
320 missions.

321 It is also worth mentioning that given the location of the accident, a drift under Bora conditions seems radically more
322 dangerous. The Bora is typically much colder and can, regardless of its short fetch, generate comparable marine conditions
323 in Northern Adriatic, but its direction is 60°, i.e. completely offshore in Northern Istria. Marine drift initiated in Umag (or
324 Savudrija) during the Bora would have lasted days, and possibly more than a week, if the object would get advected to join
325 Western Adriatic Current flowing southward along the Italian coast. Reliable and operational circulation models, coupled to
326 Lagrangian tools like OpenDrift, would be an invaluable decision support for any rapid rescue attempt.

327 *Author contributions.* A.F. and M.L. set up NEMO and ECWAM for the Adriatic basin. A.F. performed NEMO and ECWAM simulations.
328 S.E. and A.F. performed the OpenDrift simulations. S.E., C.R.S., D. D. and M. L. analyzed the HF radar data. M.L. devised the work plan,
329 wrote the FlowTrack code, performed FlowTrack simulations and wrote the paper. All authors contributed to the final version of the paper.

330 *Competing interests.* Authors declare no competing interests.

331 *Acknowledgements.* The authors would first and foremost like to thank the survivor of the incident, Mr. Goran Jablanov, for his willingness
332 to respond to the interview request and to reconstruct the trajectory of his drift as accurately as possible. M.L. would like to thank Jean Bidlot
333 (ECMWF) for his kind suggestions regarding the regional Adriatic setup of the ECWAM cycle 46R1 code. The authors would like to thank
334 Sašo Petan (ARSO) for providing Soča/Isonzo river runoff at Solkan station. The authors would like to thank all technicians and engineers
335 at our institutions for enabling and supporting the research work. M.L. wishes to acknowledge support of the Slovenian Research Agency
336 grant J1-9157: "Drivers that structure coastal marine microbiome with emphasis on pathogens – an integrated approach".

https://doi.org/10.5194/nhess-2019-362
Preprint. Discussion started: 6 January 2020

References

Allen, A. A. and Plourde, J. V.: Review of Leeway: Field Experiments and Implementation, Tech. rep., U. S. Coast Guard, 1999.

Breivik, Ø. and Allen, A. A.: An operational search and rescue model for the Norwegian Sea and the North Sea, Journal of Marine Systems, 69, 99 – 113, https://doi.org/https://doi.org/10.1016/j.jmarsys.2007.02.010, http://www.sciencedirect.com/science/article/pii/S0924796307000383, maritime Rapid Environmental Assessment, 2008.

Cavaleri, L., Bajo, M., Barbariol, F., Bastianini, M., Benetazzo, A., Bertotti, L., Chiggiato, J., Davolio, S., Ferrarin, C., Magnusson, L., Papa, A., Pezzutto, P., Pomaro, A., and Umgiesser, G.: The October 29, 2018 storm in Northern Italy – an exceptional event and its modeling, Progress in Oceanography, p. 102178, https://doi.org/https://doi.org/10.1016/j.pocean.2019.102178, https://www.sciencedirect.com/science/article/pii/S0079661119301089, 2019.

Craig, P. D. and Banner, M. L.: Modeling Wave-Enhanced Turbulence in the Ocean Surface Layer, Journal of Physical Oceanography, 24, 2546–2559, https://doi.org/10.1175/1520-0485(1994)024<2546:MWETIT>2.0.CO;2, https://doi.org/10.1175/1520-0485(1994)024<2546:MWETIT>2.0.CO;2, 1994.

Dagestad, K.-F., Röhrs, J., Breivik, Ø., and Ådlandsvik, B.: OpenDrift v1.0: a generic framework for trajectory modelling, Geoscientific Model Development, 11, 1405–1420, https://doi.org/10.5194/gmd-11-1405-2018, https://www.geosci-model-dev.net/11/1405/2018/, 2018.

Donlon, C. J., Martin, M., Stark, J. D., Roberts-Jones, J., Fiedler, E., and Wimmer, W.: The Operational Sea Surface Temperature and Sea Ice analysis (OSTIA), Remote Sensing of the Environment, 2012.

Egbert, G. D. and Erofeeva, S. Y.: Efficient Inverse Modeling of Barotropic Ocean Tides, Journal of Atmospheric and Oceanic Technology, 19, 183–204, https://doi.org/10.1175/1520-0426(2002)019<0183:EIMOBO>2.0.CO;2, https://doi.org/10.1175/1520-0426(2002)019<0183:EIMOBO>2.0.CO;2, 2002.

Engedahl, H.: Use of the flow relaxation scheme in a three-dimensional baroclinic ocean model with realistic topography, Tellus A, 47, 365–382, https://doi.org/10.1034/j.1600-0870.1995.t01-2-00006.x, https://onlinelibrary.wiley.com/doi/abs/10.1034/j.1600-0870.1995.t01-2-00006.x, 1995.

Fischer, C., Montmerle, T., Berre, L., Auger, L., and Ştefănescu, S. E.: A lateral boundary formulation for multi-level prediction models, Quarterly Journal of Royal Meteorological Society, 102, 1976.

Fischer, C., Montmerle, T., Berre, L., Auger, L., and Ştefănescu, S. E.: An overview of the variational assimilation in the ALADIN/France numerical weather-prediction system, Quarterly Journal of Royal Meteorological Society, 131, 2005.

Gerard, L., Piriou, J.-M., Brožková, R., Geleyn, J.-F., and Banciu, D.: Cloud and precipitation parameterization in a meso-gamma-scale operational weather prediction model, Monthly Weather Review, 137, 2009.

Gurgel, K.-W., Antonischki, G., Essen, H.-H., and Schlick, T.: Wellen Radar (WERA): a new ground-wave HF radar for ocean remote sensing, Coastal Engineering, 37, 219 – 234, https://doi.org/https://doi.org/10.1016/S0378-3839(99)00027-7, 1999.

Hackett, B., Breivik, Ø., and Wettre, C.: Forecasting the Drift of Objects and Substances in the Ocean, pp. 507–523, Springer Netherlands, Dordrecht, https://doi.org/10.1007/1-4020-4028-8_23, https://doi.org/10.1007/1-4020-4028-8_23, 2006.

Large, W. G. and Yeager, S. G.: Diurnal to Decadal Global Forcing for Ocean and Sea-Ice Models: The Data Sets and Flux Climatologies, https://nomads.gfdl.noaa.gov/nomads/forms/mom4/CORE.html, 2004.

Ličer, M., Smerkol, P., Fettich, A., Ravdas, M., Papapostolou, A., Mantziafou, A., Strajnar, B., Cedilnik, J., Jeromel, M., Jerman, J., Petan, S., Malačič, V., and Sofianos, S.: Modeling the ocean and atmosphere during an extreme bora event in northern Adriatic using one-way

https://doi.org/10.5194/nhess-2019-362
Preprint. Discussion started: 6 January 2020

and two-way atmosphere-ocean coupling, Ocean Science, 12, 71–86, https://doi.org/10.5194/os-12-71-2016, https://www.ocean-sci.net/12/71/2016/, 2016.

Madec, G.: NEMO ocean engine, Tech. rep., Institut Pierre-Simon Laplace (IPSL), https://www.nemo-ocean.eu/wp-content/uploads/NEMO_book.pdf, 2008.

Malačič, V.: Wind Direction Measurements on Moored Coastal Buoys, Journal of Atmospheric and Oceanic Technology, 36, 1401–1418, https://doi.org/10.1175/JTECH-D-18-0171.1, https://doi.org/10.1175/JTECH-D-18-0171.1, 2019.

Malačič, V., Petelin, B., and Vodopivec, M.: Topographic control of wind-driven circulation in the northern Adriatic, Journal of Geophysical Research: Oceans, 117, https://doi.org/10.1029/2012JC008063, https://agupubs.onlinelibrary.wiley.com/doi/abs/10.1029/2012JC008063, 2012.

Strajnar, B., Žagar, N., and Berre, L.: Impact of new aircraft observations Mode-S MRAR in a mesoscale NWP model, Journal of Geophysical Research: Atmospheres, 2015.